Chiral Near-Infrared Fluorophores by Self-Promoted Oxidative Coupling of Cationic Helicenes with Amines/Enamines

Bosson, Johann; Labrador Beltran, Maria Géraldine; Besnard, Céline; Jacquemin, Denis; Lacour, Jérôme

How to cite

BOSSON, Johann et al. Chiral Near-Infrared Fluorophores by Self-Promoted Oxidative Coupling of Cationic Helicenes with Amines/Enamines. In: Angewandte Chemie: International Edition, 2021, vol. 60, n° 16, p. 8733–8738. doi: 10.1002/anie.202016643

This publication URL: https://archive-ouverte.unige.ch/unige:150867
Publication DOI: 10.1002/anie.202016643

RESEARCH ARTICLE

Chiral Near-Infrared Fluorophores by Self-Promoted Oxidative Coupling of Cationic Helicenes with Amines / Enamines

Johann Bosson,*[a] Geraldine M. Labrador,[a] Céline Besnard,[b] Denis Jacquemin,*[c] and Jérôme Lacour *[a]

[a] Dr. J. Bosson, G. M. Labrador, Prof. J. Lacour
Department of Organic Chemistry
University of Geneva
Quai Ernest Ansermet 30, 1211 Geneva 4, Switzerland.
E-mail: johann.bosson@unige.ch, jerome.lacour@unige.ch
[b] Dr. C. Besnard
Laboratoire de Cristallographie
University of Geneva
Quai Ernest Ansermet 24, 1211 Geneva 4, Switzerland.
[c] Prof. D. Jacquemin
CEISAM UMR 6230, CNRS, University of Nantes, F-44000 Nantes, France
E-mail : Denis.Jacquemin@univ-nantes.fr

Supporting information for this article is given via a link at the end of the document. It contains experimental conditions, full characterizations of all new compounds (PDF); CSP-HPLC traces; UV-Vis, ECD, and fluorescence spectra; computational details. CCDC 2050126 (**3**) and 2050127 (**4**) contain the supplementary crystallographic data for this paper. These data can be obtained free of charge from The Cambridge Crystallographic Data Centre via www.ccdc.cam.ac.uk/structures. In addition, the dataset for this article can be found at the following DOI: 10.26037/yareta:6ar3rijxhfeclcold2y2mcsbhm. It will be preserved for 10 years.

Abstract: In one pot, tertiary alkyl amines are oxidized to enamines by cationic dioxa [6]helicene, which further reacts as electrophile and oxidant to form mono or bis donor-π-acceptor coupling products. This original and convergent synthetic approach provides a strong extension of conjugation yielding chromophores that absorb intensively in far-red or NIR domains (λ_{max} up to 791 nm) and fluoresce in the NIR as well (λ_{max} up to 887 nm). Intense ECD properties around 790 nm with a $|\Delta\varepsilon|$ value up to 60 M^{-1} cm^{-1} are observed. indolenine as reagent, direct oxidative C-C bond forming reactions lead to the mono and bis-methyleneindoline derivatives **3** and **4**. Absorption, and emission transitions of **2**-**4** are strongly localized in the far-red or NIR spectral ranges thanks to an efficient extension of the charge delocalization (λ_{abs} up to 791 nm, λ_{flu} up to 887 nm). Particularly strong NIR electronic circular dichroism (ECD) is noticed for **4** ($\Delta\varepsilon$ up to 60 M^{-1} cm^{-1} around 790 nm).

Introduction

Helicenes, chiral *ortho*-condensed polyaromatic derivatives, constitute a topic of general scientific interest due to their applications in analytics, biochemistry, catalysis and synthesis, physics and surface sciences.[1] Classical organic helicenes tend to absorb or emit light in the UV or blue parts of the spectrum.[2] To push optical properties to the orange/red domains and further, organometallic complexes can be prepared that effectively take advantage of the ability of metal centers to impact on molecular electronics.[3] With purely organic compounds, strong push-pull systems [4] or cationic variants of the helical derivatives [5] are required to induce effective bathochromic shifts up to the far red and possibly near infrared (NIR) domains; NIR being particularly important in biological contexts as absorption/emission properties localized in NIR allow deep-tissue penetration and visualization.[6] Herein, it is shown that even stronger redshifted optical properties can be achieved via oxidative coupling cascades of cationic dioxa [6]helicene **1** with simple diisopropylethyl amine (Hünig's base, HB) or indolenine reagents (Figure 1).[7] The one-pot multi-step coupling reactivity uses the ability of **1** to act both as electrophile and as oxidant. With HB as reactant, *in situ* oxidative formation of the corresponding enamine generates a powerful nucleophile able to proceed with the coupling and form helicene **2**. With

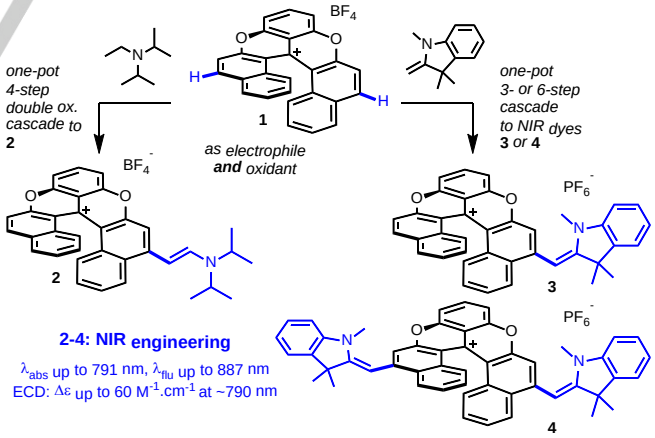

Figure 1. Access to far-red / NIR chromophores and fluorophores **2** to **4** by one-pot oxidative coupling cascades. (*P*)-enantiomers shown arbitrarily.

Results and Discussion

Previously, it was shown that triaryl carbenium ion **5** reacts with indoles to generate, in a single step, products **6** of direct oxidative coupling; carbocation **5** reacting as an electrophile but also as an oxidant (Figure 2).[7a] Of importance to the current study, strong

bathochromic shifts were noticed for the absorption properties upon the introduction of the indoles (λ_{max}: from 523 up to 630 nm). This original reactivity was unfortunately unique to achiral carbenium ion **5** and unknown in the cationic helicene series.

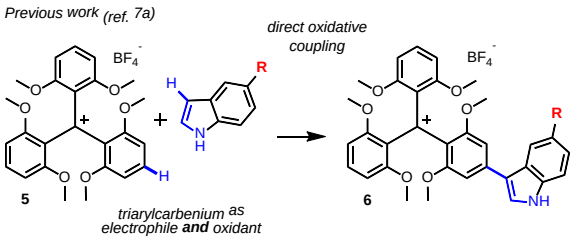

Figure 2. Direct oxidative coupling of triaryl carbenium ion **5** and indoles.

In view of the potential benefits of this synthetic approach for the generation of effective chiral NIR dyes, care was taken to find a cationic helical derivative that would present electronic properties similar to **5**. Dioxa [6]helicene **1** was rapidly identified. This compound is the most electron-poor and acidic (pK_{R+} 8.8) derivative of the cationic [n]helicene family (n=4 to 6).[5a,5b,8] As a test, **1** was treated with HB (3.0 equiv) at 90 °C in NMP (N-methyl pyrrolidinone) and, satisfactorily, functionalized [6]helicene **2** was afforded after a multistep sequence (14% isolated, 42% theoretical yield),[9] together with the reduced form **7** of the carbocation.[10] Mechanistically (Scheme 1), HB is oxidized into enamine **A** with the concomitant reduction of **1** into **7** (step 1). Such a trialkylamine oxidation is traditionally realized by a variety of methods including electron poor carbonyls,[11] Pd,[12] Pt,[13] Fe,[14] and Cu catalyzed processes,[15] metal free radical,[16] and non-radical [17] conditions.[18],[19] C-C bond formation then occurs by reaction of enamine **A** with electrophilic carbocation **1** (step 2); the reaction being totally regioselective, *para* to the formal positive charge on one of the naphthyl moiety. Resulting intermediate **B** is then oxidized to compound **C** thanks again to the presence of carbocation **1** (step 3). Finally, deprotonation occurs and cationic enamine-helicene conjugate **2** is afforded in 14% isolated or 42% theoretical yield after this multistep reaction cascade. Importantly, recycling of **7** into substrate and reagent **1** is possible. In fact, cationic **2** is readily separated from **7** by precipitation upon addition of diethyl ether to the crude reaction mixture. Remaining **7** is then dissolved in acetonitrile / dichloromethane solutions containing HBF_4 (excess) and oxidative photoirradiation (visible light, air) regenerates **1** in good isolated yield (61% from the start, step 5).[10,20] In terms of structure, detailed NMR spectroscopic analysis of **2** revealed a (*E*) configuration for the double bond; the occurrence of specific nOe cross-peaks between olefinic and helicene protons locking the geometry of the main conformation (Scheme 1, step 4).[21] This predominant structure for **2** was confirmed computationally together with a preference for the enamine and neighboring aryl ring to be almost coplanar (11.8° angle between mean plans defined by the enamine and the aryl ring, see SI); all these structural constraints pointing to an extended π-conjugation.

With this result in hand and a desire to reach NIR properties, the coupling was attempted with 1,3,3-trimethyl-2-methyleneindoline (TMI); the well-established donor character of TMI together with its enamine-type reactivity being *a priori* favorable for enhanced

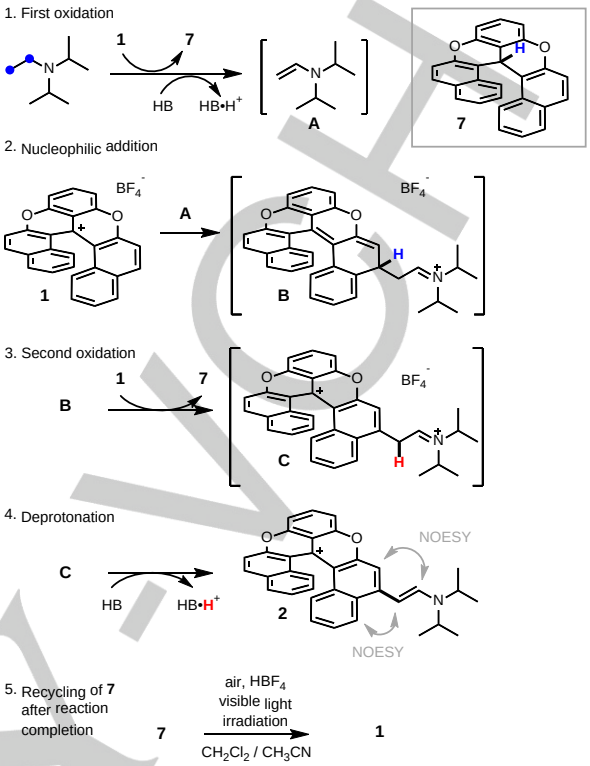

Scheme 1. Mechanistic hypothesis for the 4-step double-oxidative cascade converting **1** into **2**. 1: oxidation of the alkylamine, 2: nucleophilic addition of enamine **C**, 3: oxidation of intermediate **D** and 4: deprotonation of intermediate **E**. Reaction conditions: **1** (0.1 mmol), HB (3 equiv), NMP (0.1 M), 90 °C, 1 h, **2** isolated in 14% (42% theoretical) yield. 5: recycling of the reduced **7** into **1** (61% from start). Reaction conditions: visible light, air, 1 M aq HBF_4, CH_2Cl_2, CH_3CN (1:1:1), 3 h, 20 °C, 61% of **1** recovered. (*P*)-enantiomers shown.

properties and a more direct coupling pathway. In fact, using conditions similar to that above detailed, reaction of **1** and TMI (3 equiv) afforded mono- and bis-addition products **3** and **4** (MS monitoring); only **3** being isolated in moderate yield (10%). Optimization of reaction conditions were pursued to achieve the formation of **3** and **4** in 55% and 17% isolated yields, respectively (Figure 3). Benzophenone is an effective solvent for this class of cationic derivatives and for such transformations; reaction stoichiometry and addition of $Al(O^iPr)_3$ controlling the selectivity of the reactions towards **3** or **4** selectively.[22],[23] Satisfactorily, single crystals of **3** and **4** were obtained by slow diffusion of 1,4-dioxane in dichloromethane or chloroform solutions which were analyzed by X-ray diffraction (see SI). In the solid state, the trifling bond length alternations (BLA 0.032(6) and 0.009(8) Å for **3** and **4**, respectively) indicate an extended conjugation from the indolenine to the helicene in **3**, and between the two indolenines through the helicene core in **4** (see Figure S23 and S25), both typical of cyanine-like systems. Out-of-plane twisting of the indolenines relative to the helicenes is also observed (41.2(5)° for **3**, 40.3(7)° for **4**). In solution, the Z configuration of the double bonds in compound **3** and **4** was confirmed by ^1H NMR spectroscopy. Computational structural analyses of **2**, **3** and **4**, optimized in acetonitrile solution as implicit solvent, were performed. Several conformers of similar energies were found by

theory (see SI), reproducing well the out-of-plane twisting of the connected indolenine moieties in **3** and **4** (P_{TMI} or M_{TMI}). As such, for compound **3** and considering a *P* helicity for the helicene core (Figure 3), two predominant conformers can be identified, namely (P_{hel}-P_{TMI})-**3** and (P_{hel}-M_{TMI})-**3**. Of interest, the crystal structure of **3** yields the former structure, that DFT predicts to be only 0.08 kcal.mol^{-1} more stable than its M_{TMI} counterpart (Figure S22). Similarly, for (*P*)-**4**, three conformers were found: (P_{TMI}-P_{hel}-M_{TMI})-**4**, (P_{TMI}-P_{hel}-P_{TMI})-**4** and (M_{TMI}-P_{hel}-M_{TMI})-**4**. The conformers could not be distinguished by NMR spectroscopy. In addition, all are very close in energy according to DFT (see Figure S24), and their occurrence will have a dramatic impact on the chiroptical properties (*vide infra*). For selected examples, results are presented in Table 1 and compared with solid-state data (see also Figures S21, S23 and S25). *In silico*, helical pitches of **2**, **3**, and **4** are almost identical; calculated values being slightly larger than that measured by X-ray for **3** and **4**.[24]

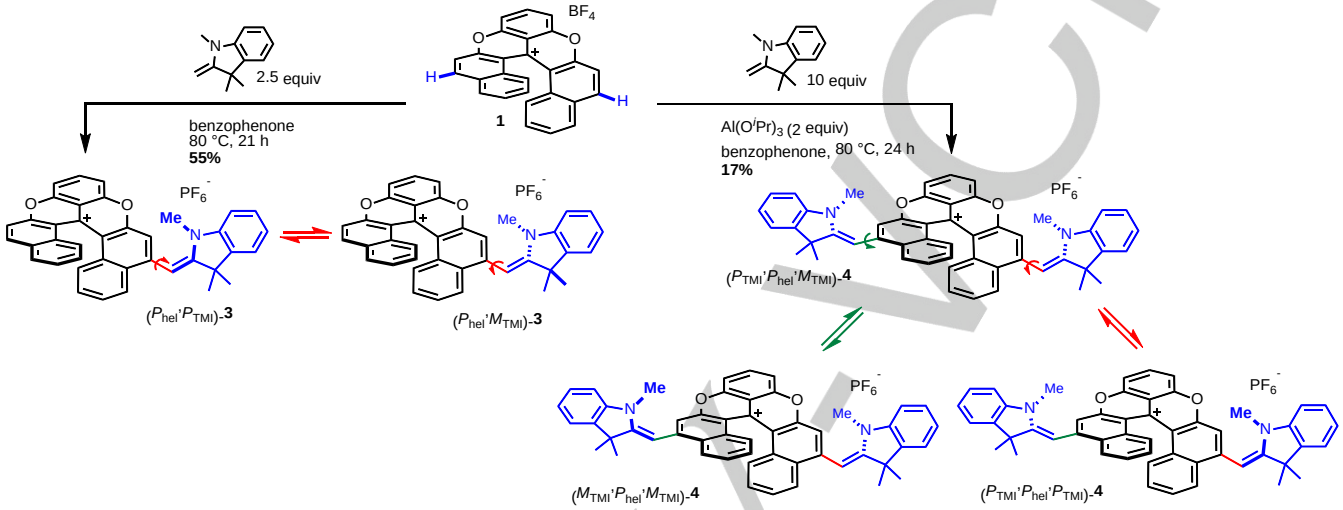

Figure 3. Oxidative addition(s) of TMI and selective formation of **3** and **4**. Considering a *P* helicity for the helicene core in compounds **3** and **4**, the TMI group(s) can adopt, in one case, two orientations named (P_{hel}-P_{TMI})-**3** and (P_{hel}-M_{TMI})-**3** and, in the other, three conformations named (M_{TMI}-P_{hel}-M_{TMI})-**4**, (P_{TMI}-P_{hel}-P_{TMI})-**4** and (P_{TMI}-P_{hel}-M_{TMI})-**4**.

Table 1. Key geometrical parameters for **2**, **3**, and **4**, considering the conformers the closest from solid state.

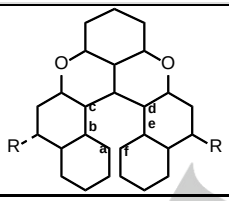

Helicene	Dihedral angle [a]		Helical pitch [b]	
	X-ray	DFT [c]	X-ray	DFT [c]
2		40.6°		3.07 Å
3	37.9(5)°	40.5°	2.941(6) Å	3.04 Å
4	41.4(6)°	38.7°	2.957(5) Å	3.04 Å

[a] the dihedral angle is defined by the torsion angle b-c-d-e. [b] the helical pitch is defined by the distance a-f. [c] the values correspond to the computed data (M06-2X/6-31+G(d), PCM=Acetonitrile, see SI).

The electronic character of **2**, **3**, and **4** was investigated by cyclic voltammetry and the results compared to parent **1** (Figure 4 and Table 2). As expected, the presence of the enamine motifs renders all substituted derivatives more electron-rich than **1**. Pseudo-reversible reductions occurred at –0.48, –0.31 and –0.39 V *vs.* Ag for **2**, **3**, and **4**, respectively (instead of –0.12 V for **1**).[5b,25] Somewhat surprisingly, this also indicates a lower electron-donating contribution of the indolenine moieties as compared to the diisopropylenamine; compound **2** being quite more difficult to reduce than **3** and even **4**.[26] In oxidation mode, a more intuitive trend was observed since non-reversible signatures were found at +1.02 and +0.97 V for **2** and **3**, respectively; the electron-rich nature of the indolenine outpacing that of the enamine. With **4**, two waves were found at +0.79 and +1.11 V *vs.* Ag, respectively. This indicates that the two indolenine substituents are oxidized sequentially. It implies furthermore that the donor moieties are electronically connected thus confirming the electronic conjugation over the whole structure, a fact further ascertained with theory (*vide infra*).

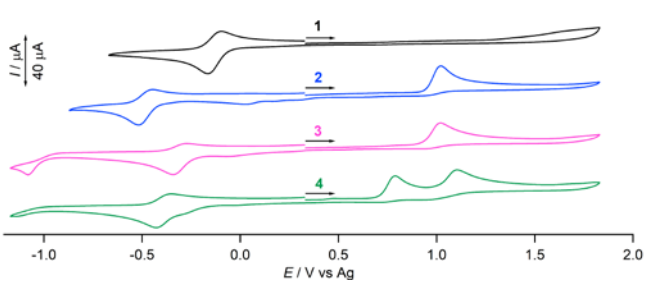

Figure 4. Cyclic voltammograms of **1** to **4** recorded in degassed CH_3CN solution (C = 10^{-3} M) containing 0.1 M [Bu_4N][PF_6] as supporting electrolyte. Scan rate 0.1 V s^{-1}. The potentials are referred to Ag.

The optical properties of **2**, **3**, and **4** were next investigated in acetonitrile solutions (Figure 5, A and B and Table 2). As expected,

in comparison with **1** (λ_{abs} 562 nm, λ_{em} 594 nm), strong bathochromic and hyperchromic shifts were observed for **2**.[5b] At lower energy, the intense absorption band presents two maxima at 639 and 687 nm (ε 46400 and 45200 M^{-1} cm^{-1} for the 0-1 and 0-0 sub-bands, respectively).[27] The electron density difference plots for **1**, **2**, **3**, and **4** are displayed in Figure 5C. One clearly notes the hallmark cyanine character in all cases, with alternance of gain (loss) of density on the odd (even) carbon atoms in the conjugation path and a strong increase of density on the central carbon center. More importantly, the extended delocalization of excited-state onto the indolenine moieties is obvious, which explains the observed red-shifts. In addition, compound **2** fluoresces in the NIR with a broad emission band centered on 807 nm, albeit with a weak efficiency (ϕ_{flu} < 1%), which is likely related to very redshifted character of the fluorescence (*energy gap law*). Further redshifts were noticed for **3** with a lower energy absorption transition centered on 727 nm (ε 41000 M^{-1} cm^{-1}) and a fluorescence in the NIR with a maximum peaking at 823 nm; this luminescence being however too weak to be quantified. Product **4** possesses both the lowest energy transition and its allied fluorescence in the NIR, with an intense absorption band centered on 791 nm (ε 84600 M^{-1} cm^{-1}) and λ_{em} around 900 nm also very weak. The Stokes shifts reported in Table 2 are typical of organic fluorophores, with a significant increase from **1** to **2** and intermediate values for **3** and **4**, which follows chemical intuition as **2** presents the less rigid substituent. All these properties, including the cyclic voltammetry results, are summarized in Table 2. Comparisons with CC2 and TD-DFT theoretical values can be found in the SI (Table S13) and theory is found to reproduce the trends in both 0-0 energies and absorption intensity in the **1** - **4** series.

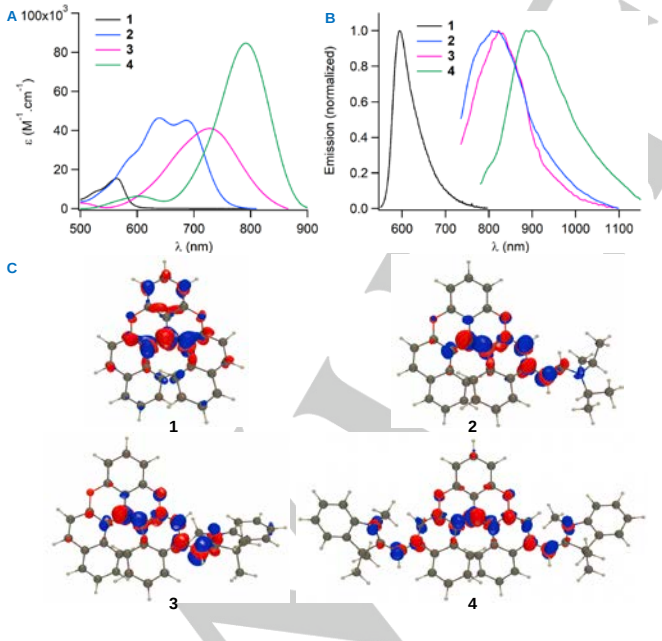

Figure 5. A: absorption and B: normalized fluorescence spectra of helicenes **1** (black), **2** (blue), **3** (pink) and **4** (green) in acetonitrile (C *ca.* 10^{-5} M). C: electron density difference plots for **1**, **2**, **3** and **4**,(isovalues: 0.002 au). In the latter, the blue and red regions represent decrease and increase of density upon absorption, respectively.

Previously, it was shown that dioxa [6]helicene **1** does not exhibit significant solvatochromism.[5b] However, as absorption properties present typical merocyanine, for **2**, and cyanine characters, for **3** and **4**, the influence of solvent on their optical properties was scrutinized. Globally, in the series, weak negative solvatochromism was observed in protic and aprotic solvent series. For instance, for **2**, λ_{abs} spans from 679 nm to 689 nm from CF_3CH_2OH to CH_3OH (considering the most redshifted band, see Figures S10 and S11).[28] For **3** (Figures S12 and S13), absorption maxima shift to low energy from 721 (CF_3CH_2OH) to 730 nm (CH_3CH_2OH) and from 727 (CH_3CN) to 743 nm ($CHCl_3$). In an analogously manner for **4**, absorption maxima changes from 779 to 799 nm in alcoholic solvents; the lowest energy transition being observed at 811 nm in $CHCl_3$ (Figures S14 and S15). These rather trifling solvatochromic effects are well in line with the theoretical calculations that predict rather small changes of dipole moments between the ground and the excited states, the absolute variations being typically on the 1-2 D window in the **1** - **4** series.

Table 2. Optical and electronic characterization of **1** to **4**.

	λ_{abs} [a]	ε [b]	λ_{flu} [a]	Stokes shift [c]	$E_{1/2}^{red}$ [d]	E^{ox} [d]
1	562	15000	594	959	–0.12	+2.14
2 [e]	687	45200	807	2164	–0.48	+1.02
3	727	41000	823	1642	–0.31	+0.97
4	791	84600	887	1368	–0.39	+0.79 +1.11

Absorption and fluorescence spectra, and cyclic voltammograms were recorded in acetonitrile solutions.[a] in nm. [b] in M^{-1} cm^{-1}. [c] in cm^{-1}. [d] pseudo-reversible reduction and non-reversible oxidation waves, in V *vs.* Ag. [e] For **2**, values correspond to the most redshifted band.

Finally, chiroptical ECD properties of helicenes **2** to **4** were studied. The enantiomers were separated by chiral stationary phase (CSP) HPLC. Despite structural similarities, three different CSP were necessary to achieve effective separations. Compound **2** was resolved using cyclofructan-based LARIHC,[29] **3** using CHIRALPAK® IC and **4** with CHIRALCEL® OJ-H (see SI). Then, with the single enantiomers in hand, the ECD spectra of helicenes **2** to **4** were recorded in acetonitrile (Figure 6).[30] In the UV domain, strong signals are observed around 220 nm, |Δε| = 130-150 M^{-1} cm^{-1}, and at ~270 nm, |Δε| = 70-95 M^{-1} cm^{-1}.[31] The sign and intensity of the bands are fully conserved for the levo and dextrorotatory enantiomers of **2**, **3** and **4**, indicative of identical absolute configurations for the (–) and (+)-enantiomers in this series. Then, with the help of the reactivity of **2** with TFA that leads to the deconjugated iminium species **2·H⁺** (see SI for the characterization of the reversible protonation pathway), absolute configuration assignment was achieved by ECD comparison of (–)-**2·H⁺** with (–)-(*M*)-**1**, and (+)-**2·H⁺** with (+)-(*P*)-**1** that presents virtually identical ECD spectra (Figure S19).[8] The levo and dextrorotatory enantiomers of **2**, **3** and **4** are therefore of *M* and *P* configurations respectively. For the lowest energy transition, (–)- and (+)-**2** exhibited large Cotton effect from 620 to 720 nm, |Δε| ~ 10 M^{-1} cm^{-1}.[32] For this derivative, theory finds a strongly dominant conformer for which TD-DFT returns a rather similar |Δε| of 19 M^{-1} cm^{-1} (Table S13), with the same sign as in the experiment, i.e., -19 M^{-1} cm^{-1} for the P_{hel}, a consistency also holding for **3** and **4**. Also in the far-red, compound **3** exhibited a strong chiroptical

signature for the lowest transition, |Δε| between 10 and 15 M^{-1} cm^{-1} from 650 to 770 nm. As mentioned for this derivative, theory finds two conformers that are compatible with NMR measurements (*s-cis* conformation, see ref. 21) and are almost isoenergetic (ΔG° 0.08 kcal.mol^{-1}, see Figure 3 and S22). As can be seen in Table S13, the computed ε of these two structures are very similar (42 and 40 x 10^3 $M^{-1}cm^{-1}$, very close to the measured values displayed in Table 2), but the Δε corresponding to the lowest excited-state are strongly different: -4 (P_{hel}-M_{TMI}) and -31 (P_{hel}-P_{TMI}) M^{-1} cm^{-1}, the experimental values being the rough average between these two values. This clearly hints that several conformers of significantly different chiroptical responses are likely present in solution. Finally, intense low energy bands were observed for **4**. A strong Cotton effect is associated to the $S_0 \rightarrow S_2$ transition with a band peaking at 600 nm, |Δε| = 30 M^{-1} cm^{-1}. Yet, the strongest effect is observed in the NIR for the lowest energy transition which presents a remarkable signature around 790 nm with a |Δε| value up to 60 M^{-1} cm^{-1}. For **4**, theory returns three *s-cis* conformers within 1 kcal.mol^{-1} though the difference in free energy is now more marked than for **3** (Figure S24). For these three conformers, the computed absorption and emission properties are very alike, but the rotatory strengths significantly differ with Δε of -66, -6 and -35 M^{-1} cm^{-1}, for (P_{TMI}-P_{hel}-P_{TMI})-**4**, (M_{TMI}-P_{hel}-M_{TMI})-**4**, and (P_{TMI}-P_{hel}-M_{TMI})-**4**, respectively (Table S13). A Boltzmann distribution of the three conformers (based on the DFT free energies yield weights of 64%, 19%, and 17%, providing an averaged Δε of -49 M^{-1} cm^{-1}, again reasonably in line with the measurement. Besides showing that the experimental response likely comes from several conformers as in **3**, it is interesting to note that the conformer observed in the solid state, *i.e.* (M_{TMI}-P_{hel}-M_{TMI})-**4,** is the one leading to the smallest response of the three isomers (|Δε| of 6 M^{-1} cm^{-1}), so that it is unlikely to be dominant in solution.

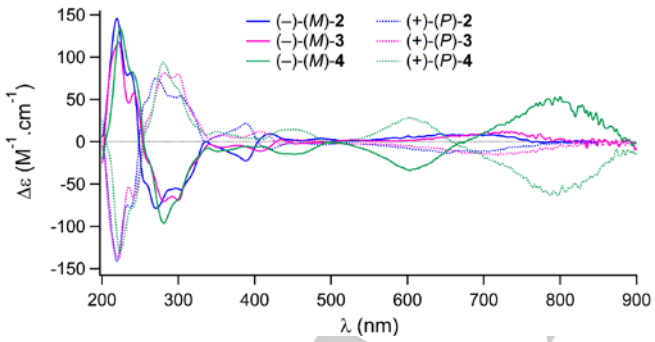

Figure 6. ECD spectra of the (–)-(*M*) (plain line) and (+)-(*P*)-enantiomers (dashed lines) of **2** (blue), **3** (pink) and **4** (green) in acetonitrile solutions.

Conclusion

Cationic dioxa [6]helicene **1** readily oxidizes tertiary alkyl amines such as HB into the corresponding enamine. Then, nucleophilic oxidative addition of such *in situ* generated intermediate onto **1** leads to the formation of merocyanine-like products of type **2**. With TMI as nucleophile, mono- and bis-addition products of oxidative coupling **3** and **4** are selectively prepared. Due to the extension of the π-delocalization, the optical properties of **2** to **4** display very strong hyper and bathochromic shifts as compared to **1**. These salts, that absorb in far-red or NIR domains (λ_{max} up to 791 nm) and fluoresce in the NIR (λ_{max} up to 887 nm), are rare examples of helicenes displaying chiroptical properties in the NIR.[33] Strong ECD signals are noted, up to |Δε| = 60 M^{-1} cm^{-1} around 800 nm for the most red-shifted derivative. TD-DFT analyses indicate that several conformers are likely involved in the chiroptical response of **3** and **4**.

Acknowledgements

We thank the University of Geneva and the Swiss National Science (SNF grants 200020-172497 and 200020-184843) for funding and support. Dr. Pilar Franco and Dr. Assunta Green (Chiral Technologies Europe) and Stéphane Grass (Geneva) are warmly thanked for their crucial help in the CSP-HPLC resolutions. The help of Dr. Alexandre Fürstenberg (UNIGE) for the low energy fluorescence spectra measurements is greatly acknowledged. The support of Dr. Amalia I. Poblador-Bahamonde and Carmine Chiancone (UNIGE) for the computational study is highly appreciated. D.J. is indebted to the CCIPL computational center installed in Nantes for generous allocations of computational resources.

Keywords: Helicenes • NIR dyes and fluorophores • TD-DFT • cyanines • oxidative coupling cascades

[1] a) M. Gingras, *Chem. Soc. Rev.* **2013**, *42*, 1051-1095; b) P. Aillard, A. Voituriez, A. Marinetti, *Dalton Trans.* **2014**, *43*, 15263-15278; c) J. Bosson, J. Gouin, J. Lacour, *Chem. Soc. Rev.* **2014**, *43*, 2824-2840; d) N. Saleh, C. Shen, J. Crassous, *Chem. Sci.* **2014**, *5*, 3680-3694; e) H. Isla, J. Crassous, *C. R. Chim.* **2016**, *19*, 39-49; f) M. Shigeno, Y. Kushida, M. Yamaguchi, *Chem. Commun.* **2016**, *52*, 4955-4970; g) C.-F. Chen, Y. Shen, *Helicene Chemistry From Synthesis to Applications*, Springer, Berlin, Heidelberg, **2017**; h) I. Stary, I. G. Stara, *Targets Heterocycl. Syst.* **2017**, *21*, 23-53; i) K. Dhbaibi, L. Favereau, J. Crassous, *Chem. Rev.* **2019**, *119*, 8846-8953; j) K. Kato, Y. Segawa, K. Itami, *Synlett* **2019**, *30*, 370-377; k) W.-L. Zhao, M. Li, H.-Y. Lu, C.-F. Chen, *Chem. Commun.* **2019**, *55*, Ahead of Print.

[2] E. Van der Donckt, J. Nasielski, J. R. Greenleaf, J. B. Birks, *Chem. Phys. Lett.* **1968**, *2*, 409-410.

[3] a) J. OuYang, J. Crassous, *Coord. Chem. Rev.* **2018**, *376*, 533-547; b) E. S. Gauthier, R. Rodriguez, J. Crassous, *Angew. Chem., Int. Ed.* **2020**, Ahead of Print.

[4] a) M. Li, Y. Niu, X. Zhu, Q. Peng, H.-Y. Lu, A. Xia, C.-F. Chen, *Chem. Commun.* **2014**, *50*, 2993-2995; b) M. Li, W. Yao, J.-D. Chen, H.-Y. Lu, Y. Zhao, C.-F. Chen, *Journal of Materials Chemistry C* **2014**, *2*, 8373-8380; c) M. Li, H.-Y. Lu, C. Zhang, L. Shi, Z. Tang, C.-F. Chen, *Chem. Commun.* **2016**, *52*, 9921-9924; d) Z.-H. Zhao, X. Liang, M.-X. He, M.-Y. Zhang, C.-H. Zhao, *Org. Lett.* **2019**, *21*, Ahead of Print; e) S. K. Pedersen, K. Eriksen, M. Pittelkow, *Angew. Chem. Int. Ed.* **2019**, *58*, 18419-18423; f) K. Dhbaibi, L. Favereau, M. Srebro-Hooper, C. Quinton, N. Vanthuyne, L. Arrico, T. Roisnel, B. Jamoussi, C. Poriel, C. Cabanetos, J. Autschbach, J. Crassous, *Chem. Sci.* **2020**, *11*, 567-576.

[5] a) F. Torricelli, J. Bosson, C. Besnard, M. Chekini, T. Bürgi, J. Lacour, *Angew. Chem. Int. Ed.* **2013**, *52*, 1796-1800; b) J. Bosson, G. M. Labrador, S. Pascal, F.-A. Miannay, O. Yushchenko, H. Li, L. Bouffier, N. Sojic, R. C. Tovar, G. Muller, D. Jacquemin, A. D. Laurent, B. Le Guennic, E. Vauthey, J. Lacour, *Chem. Eur. J.* **2016**, *22*, 18394-18403; c) I. H. Delgado, S. Pascal, A. Wallabregue, R. Duwald, C. Besnard, L. Guenee, C. Nancoz, E. Vauthey, R. C. Tovar, J. L. Lunkley, G. Muller, J. Lacour, *Chem. Sci.* **2016**, *7*, 4685-4693; d) R. Duwald, S. Pascal, J. Bosson, S. Grass, C. Besnard, T. Buergi, J. Lacour, *Chem. - Eur. J.* **2017**, *23*, 13596-13601; e) R. Duwald, J. Bosson, S. Pascal, S. Grass, F. Zinna, C. Besnard, L. Di Bari, D. Jacquemin, J. Lacour, *Chem. Sci.* **2020**, *11*, 1165-1169.

[6] S. Wang, B. Li, F. Zhang, *ACS Central Science* **2020**.

[7] a) R. Vanel, F.-A. Miannay, E. Vauthey, J. Lacour, *Chem. Commun.* **2014**, *50*, 12169-12172; b) D. Wang, X. Guo, H. Wu, Q. Wu, H. Wang, X. Zhang, E. Hao, L. Jiao, *J. Org. Chem.* **2020**, *85*, 8360-8370.

[8] G. M. Labrador, C. Besnard, T. Burgi, A. I. Poblador-Bahamonde, J. Bosson, J. Lacour, *Chem. Sci.* **2019**, *10*, 7059-7067.

[9] As compound **1** reacts twice as an oxidant and only once as an electrophile, the maximum isolated yield is 33% only.

[10] G. M. Labrador, J. Bosson, Z. S. Breitbach, Y. Lim, E. R. Francotte, R. Sabia, C. Villani, D. W. Armstrong, J. Lacour, *Chirality* **2016**, *28*, 282-289.

[11] a) R. R. Fraser, R. B. Swingle, *Tetrahedron* **1969**, *25*, 3469-3475; b) S. L. Schreiber, *Tetrahedron Lett.* **1980**, *21*, 1027-1030; c) J. J. Talley, *Tetrahedron Lett.* **1981**, *22*, 823-826.

[12] a) Z. Huang Yao, Q. Zhou, *J. Org. Chem.* **1987**, *52*, 3552-3558; b) A. Morigaki, M. Kawamura, S. Arimitsu, T. Ishihara, T. Konno, *Asian J. Org.Chem.* **2013**, *2*, 239-243.

[13] X.-F. Xia, X.-Z. Shu, K.-G. Ji, Y.-F. Yang, A. Shaukat, X.-Y. Liu, Y.-M. Liang, *J. Org. Chem.* **2010**, *75*, 2893-2902.

[14] N. Takasu, K. Oisaki, M. Kanai, *Org. Lett.* **2013**, *15*, 1918-1921.

[15] M.-J. Zhou, S.-F. Zhu, Q.-L. Zhou, *Chem. Commun.* **2017**, *53*, 8770-8773.

[16] R. J. Griffiths, W. C. Kong, S. A. Richards, G. A. Burley, M. C. Willis, E. P. A. Talbot, *Chem. Sci.* **2018**, *9*, 2295-2300.

[17] a) K. Kiyokawa, T. Kosaka, T. Kojima, S. Minakata, *Angew. Chem. Int. Ed.* **2015**, *54*, 13719-13723; b) H. Jiang, X. Tang, Z. Xu, H. Wang, K. Han, X. Yang, Y. Zhou, Y.-L. Feng, X.-Y. Yu, Q. Gui, *Org. Biomol. Chem.* **2019**, *17*, 2715-2720.

[18] J. Choi, A. H. R. MacArthur, M. Brookhart, A. S. Goldman, *Chem. Rev.* **2011**, *111*, 1761-1779.

[19] Enamines are also generated in photoredox processes using trialkylamines as sacrificial electron donors, see a) A. Romero, D. A. Nicewicz, *Chem. Rev.* **2016**, *116*, 10075-10166; b) J.-R. Chen, X.-Q. Hu, L.-Q. Lu, W.-J. Xiao, *Chem. Soc. Rev.* **2016**, *45*, 2044-2056; c) J. Hu, J. Wang, T. H. Nguyen, N. Zheng, *Beilstein J. Org. Chem.* **2013**, *9*, 1977-2001.

[20] S. Yokoyama, T. Hirose, K. Matsuda, *Chem. Lett.* **2015**, *44*, 76-78.

[21] Using the Kekule representation of **2** in Scheme 1, the *s-cis* conformation is the only one observed in the ^{1}H NMR spectra at room temperature. This analysis holds for **3** and **4**.

[22] Hydride abstraction by the benzophenone in an Oppenauer-like oxidation has been mechanistically considered even if benzhydrol could not be detected in the reaction mixture.

[23] Under these conditions, recovery of leuco adduct **7**, or its oxidation to starting material **1** after reaction completion, could not be achieved readily.

[24] This flattening of the helicenes in the solid state may be due to intermolecular packing interactions.

[25] a) H. Li, A. Wallabregue, C. Adam, G. M. Labrador, J. Bosson, L. Bouffier, J. Lacour, N. Sojic, *J. Phys. Chem. C* **2017**, *121*, 785-792; b) H. Li, S. Voci, A. Wallabregue, C. Adam, G. M. Labrador, R. Duwald, I. Hernández Delgado, S. Pascal, J. Bosson, J. Lacour, L. Bouffier, N. Sojic, *ChemElectroChem* **2017**, *4*, 1750-1756.

[26] A second mono electronic non-reversible reduction leading to the neutral helicene happens at –1.08 V vs. Ag.

[27] H. Mustroph, A. Towns, *ChemPhysChem* **2018**, *19*, 1016-1023.

[28] A. V. Kulinich, E. K. Mikitenko, A. A. Ishchenko, *Phys. Chem. Chem. Phys.* **2016**, *18*, 3444-3453.

[29] P. Sun, C. Wang, Z. S. Breitbach, Y. Zhang, D. W. Armstrong, *Anal. Chem.* **2009**, *81*, 10215-10226.

[30] Cationic [6]helicenes are highly configurationally stable derivatives presenting racemization barriers from 29.8 to >37 kcal/mol. In compounds **2**-**4**, the added electron-donor group(s) likely increase the configurational stability of the derivatives in addition. See reference [10].

[31] Y. Nakai, T. Mori, Y. Inoue, *J. Phys. Chem. A* **2013**, *117*, 83-93.

[32] Preliminary CPL measurement was attempted with (–)-**2** and (+)-**2**. Unfortunately, the signal was below detection limits ($g_{lum} < 10^{-4}$), in line with the relatively weak g_{abs} value ($7\ 10^{-4}$). See H. Tanaka, Y. Inoue and T. Mori, *ChemPhotoChem*, **2018**, *2*, 386-402.

[33] T. Mori, *Circularly Polarized Luminescence of Isolated Small Organic Molecules*, Springer, Singapore, **2020**.

Entry for the Table of Contents

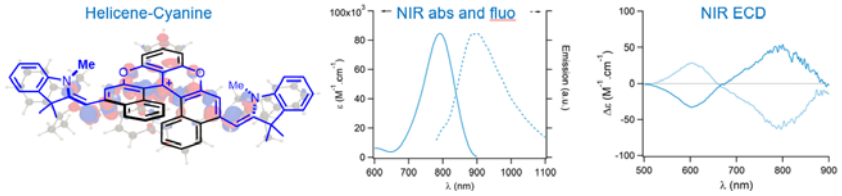

Cationic dioxa [6]helicene oxidizes alkyl amines to enamines and further reacts *in-situ* as an electrophile to form, in one-pot multi-step cascades, fully delocalized mono or bis donor-π-acceptor coupling products. This original approach provides chiral cyanine-like chromophores that absorb up to the NIR and fluoresce alike, with intense NIR ECD (Δε up to 60 M^{-1} cm^{-1}). DFT showcases the importance of conformers in the strong chiroptical response.

Institute and/or researcher Twitter usernames: @UniGe_OrgChem @CeisamLab @johannbosson @LACOUR_UNIGE